Theoretical modelling and numerical simulation of seismic motions at seafloor

Chao Li[1, 2, *], Hong Hao[2], Hongnan Li[1] and Kaiming Bi[2]
[1]*Faculty of Infrastructure Engineering, Dalian University of Technology, Dalian 116024, China*
[2]*Centre for Infrastructure Monitoring and Protection, School of Civil and Mechanical Engineering, Curtin University, Kent Street, Bentley WA 6102, Australia*

Abstract: This paper proposes a modelling and simulation method of seafloor seismic motions on offshore sites, which are composed of the base rock, the porous soil layers and the seawater layer, based on the fundamental hydrodynamics equations and one-dimensional wave propagation theory. The base rock motions are assumed to consist of P- and S-waves and are modelled by the seismological model in southwest of Western Australia (SWWA). The transfer functions of the offshore site are calculated by incorporating the derived dynamic-stiffness matrix of seawater layer into the total stiffness matrix. The effect of water saturation on the P-wave velocity and Poisson's ratio of subsea soil layers are considered in the model. Both onshore and seafloor seismic motions are stochastically simulated. The comparison results show that the seafloor vertical motions are significantly suppressed near the P-wave resonant frequencies of the upper seawater layer, which makes their intensities much lower than the onshore vertical motions. The simulated seafloor motions are in compliance with the characteristics of available seafloor earthquake recordings and can be used as inputs in the seismic analyses of offshore structures.
Keywords: seafloor motion simulation; seawater layer; wave propagation theory; transfer function

1. Introduction

Due to the insufficiency of seafloor earthquake recordings and the lack of methodologies to predict seafloor seismic motions, onshore motions are commonly used as inputs in the seismic analyses of offshore structures. This may lead to erroneous structural response predictions since the seafloor seismic motions may be very different from the onshore ones. The effect of seawater layer on the seafloor motions has been investigated by a few researchers through theoretical calculations [1, 2] or statistical analyses of actual seafloor earthquake recordings [2, 3]. These studies indicated that the vertical-to-horizontal (V/H) PGA and spectral ratios of the seafloor seismic motions are much lower than those of the onshore motions, owing to the significant suppression effect of seafloor vertical motions near the P-wave resonant frequencies of the seawater layer.

Moreover, the seawater layer can indirectly influence the seafloor motions by changing the water saturation and pore pressure of subsea soil layers, which can significantly affect the propagation of seismic P-waves in the offshore site. Many studies have been carried out to investigate the dynamic behavior of fully saturated [4, 5] and nearly saturated [6] porous soils. Base on the concept of homogeneous pore fluid [7] and Biot's theory for wave propagation in two phase media [4, 5], Yang and Sato [8] studied the effects of degree of saturation on the P-wave velocity and Poisson's ratio of the soil layers; Wang and Hao [9] examined the influence of ground water level on the propagation of seismic waves. Both of these two studies [8, 9] demonstrated that the site amplification effect of vertical seismic motions can be significantly influenced by the saturation degree of soil layers.

*Corresponding author. Tel: +61 452121917. E-mail address: lichao17007@163.com (C. Li).

By considering the effects of seawater layer and water saturation of subsea soil layers on the site amplification of seismic waves, a simulation method of seafloor seismic motions is proposed in this paper. The offshore site transfer functions are theoretically derived by utilizing the fundamental hydrodynamics equations [10, 11] and one-dimensional wave propagation theory [12]. Onshore and seafloor seismic motions are both stochastically simulated based on the base rock motion, which is represented by the seismological model of southwest of Western Australia (SWWA) [13] and the corresponding site transfer functions. The differences between the characteristics of simulated onshore and seafloor seismic motions are discussed. It should be noted that the seismic surface waves may also be affected by the seawater layer [14], however, since they are generally neglected in engineering practice, the simulation of surface waves is not in the scope of this study.

2. Dynamic-stiffness matrix of seawater layer

In this study, the seawater is assumed as an ideal fluid in which only seismic P-waves can propagate. The fluid motion can be expressed with the conservation equation of mass, the Euler's equation and the adiabatic equation of state [10], from which the linear wave equation of seismic P-waves in seawater can be derived as [15]

$$\nabla^2\psi - \frac{1}{c_p^2}\frac{\partial^2\psi}{\partial t^2} = 0 \tag{1}$$

where ψ is the displacement potential defined by $\boldsymbol{u}=\nabla\psi$, with $\boldsymbol{u}$ denoting the displacement vector of the fluid particle; ∇^2 is the Laplace operator; c_p is the seismic P-wave velocity, which is defined as

$$c_p^2 = \frac{K}{\rho} \tag{2}$$

where K and ρ are the bulk modulus and density of seawater, respectively.

For a harmonic seismic P-wave excitation with circular frequency ω, the linear wave equation can be expressed with the Helmholtz equation [16]

$$\nabla^2\psi + \frac{\omega^2}{c_p^2}\psi = 0 \tag{3}$$

Based on the conservation equation of mass and the adiabatic equation of state, the fluid pressure p induced by seismic P-waves can be derived as [15]

$$p = -K\nabla^2\psi \tag{4}$$

In the classical fluid dynamics [11], all the stress tensors of Newtonian fluid in the Cartesian coordinates can be expressed as

$$\sigma_{ij} = -p_f\delta_{ij} + \mu\left[\left(\frac{\partial v_i}{\partial x_j} + \frac{\partial v_j}{\partial x_i}\right) - \frac{2}{3}\delta_{ij}\nabla\cdot\boldsymbol{v}\right] \tag{5}$$

where μ denotes the fluid viscosity; δ_{ij} equals 1 when i=j and 0 when i≠j; p_f denotes the average normal compressive stress and can be interpreted as a scalar acting on the surface of an infinitesimal fluid particle. For the ideal fluid assumed in this study, μ equals zero and only the first part, i.e., the normal stress part in Eq. (5) remains. Additionally, p_f can be replaced with the earthquake induced fluid pressure p as expressed in Eq. (4).

The one-dimensional wave propagation theory presented by Wolf [12] can be used to calculate the dynamic-stiffness matrices of base rock and soil layers. By combining the hydrodynamics equations presented above, Wolf's approach is employed in this study to

derive the dynamic-stiffness matrix of seawater layer. The wave equation, i.e., Eq. (3) can be solved with the P-wave trail function:

$$\psi = A_p \exp\left[\frac{i\omega}{c_p}\left(-l_x x - l_y y - l_z z\right)\right] \tag{6}$$

where A_p denotes the P-wave amplitude; l_x, l_y and l_z are the propagation direction cosines in the Cartesian coordinates. Eq. (3) is satisfied when

$$l_x^2 + l_y^2 + l_z^2 = 1 \tag{7}$$

Substituting Eq. (6) into $\boldsymbol{u}=\nabla\psi$ and Eqs. (4) and (5), the fluid particle displacement vectors and normal stresses under P-wave excitation can be obtained by taking the material damping of seawater into account:

$$u_n = -l_n A_p \frac{i\omega}{c_p^*}\exp\left[\frac{i\omega}{c_p^*}\left(-l_x x - l_y y - l_z z\right)\right] \tag{8}$$

$$\sigma_{nn} = -K^* A_p \frac{\omega^2}{c_p^{*2}}\exp\left[\frac{i\omega}{c_p^{*2}}\left(-l_x x - l_y y - l_z z\right)\right] \tag{9}$$

where n represents direction x, y, or z; K^* and $c_p{}^*$ are the complex values of bulk modulus and wave velocity with the fluid damping introduced.

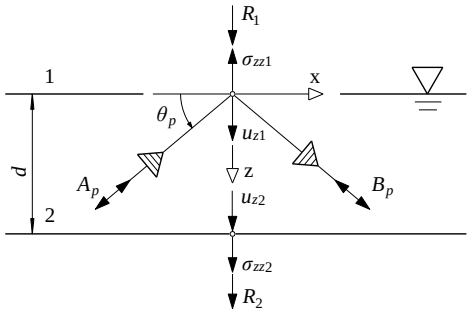

Fig. 1. Nomenclature of seawater layer for in-plane P-wave motion

Fig. 1 shows the nomenclature of seismic P-waves propagating in the seawater layer. The P-wave motion is assumed to be in-plane (x-z plane), i.e. l_y=0. Thus, $l_x{}^2+l_z{}^2=1$ is obtained from Eq. (7). The depth of seawater layer and the P-wave inclined angle are represented by d and θ_p, respectively. Since the ideal fluid cannot withstand shear stress, only the vertical displacement and stress are concerned. A reflected P-wave with amplitude B_p is introduced to satisfy the two boundary conditions of displacement and stress. Based on Eqs. (8) and (9), the vertical displacement and stress of fluid particle can be formulated as

$$u_z = \sqrt{1-l_x^2}\frac{i\omega}{c_p^*}\left[A_p \exp\left(\frac{i\omega}{c_p^*}\sqrt{1-l_x^2}\,z\right) - B_p \exp\left(-\frac{i\omega}{c_p^*}\sqrt{1-l_x^2}\,z\right)\right]\exp\left[-\frac{i\omega}{c_p^*}l_x x\right] \tag{10}$$

$$\sigma_{zz} = -K^*\frac{\omega^2}{c_p^{*2}}\left[A_p \exp\left(\frac{i\omega}{c_p^*}\sqrt{1-l_x^2}\,z\right) + B_p \exp\left(-\frac{i\omega}{c_p^*}\sqrt{1-l_x^2}\,z\right)\right]\exp\left[-\frac{i\omega}{c_p^*}l_x x\right] \tag{11}$$

The above two expressions can be simplified with the following notations:

$$c = c_p^* / l_x \tag{12}$$

$$k = \omega / c \tag{13}$$

$$s = -i\sqrt{1-1/l_x^2} \tag{14}$$

where c and k denote the phase velocity and the wave number, respectively. The value of s

equals tanθ_p.

Thus, the amplitude of P-wave propagating in the *x*-direction can be represented as

$$u_z(z) = iks\left[A_p \exp(iksz) - B_p \exp(-iksz)\right] \tag{15}$$

$$\sigma_{zz}(z) = -K^* \frac{\omega^2}{c_p^{*2}}\left[A_p \exp(iksz) + B_p \exp(-iksz)\right] \tag{16}$$

With these two equations, the vertical fluid displacement and stress at the top (z=0) and the bottom (z=d) of the seawater layer can be directly obtained. By further eliminating the amplitude items A_p and B_p and introducing the external load amplitudes R_1=−σ_{zz1} and R_2=σ_{zz2} in the global coordinate system as illustrated in Fig. 1, the dynamic-stiffness matrix of the seawater layer is derived as

$$\begin{Bmatrix} R_1 \\ R_2 \end{Bmatrix} = \left[S_P^W\right]\begin{Bmatrix} u_{z1} \\ u_{z2} \end{Bmatrix} = \frac{K^*\omega}{l_x s c_p^* \sin ksd}\begin{bmatrix} \cos ksd & -1 \\ -1 & \cos ksd \end{bmatrix}\begin{Bmatrix} u_{z1} \\ u_{z2} \end{Bmatrix} \tag{17}$$

where the subscripts 1 and 2 represent the top and bottom of the seawater layer, respectively; $[S_P^W]$ denotes the dynamic-stiffness matrix that describes the relationship between the external load and displacement at the two seawater layer boundaries.

3. Calculation of offshore site transfer functions

The transfer functions of an offshore site, which is composed of the base rock, the porous soil layers and the seawater layer, can be calculated based on the derived dynamic-stiffness matrix of seawater layer. The base rock motions are assumed to consist of out-of-plane SH-wave or in-plane combined P- and SV-waves with respective incident angles [12]. The dynamic equilibrium equation for an offshore site can be expressed in the frequency domain as

$$\left[S_{SH}\right]\{u_{SH}\} = \{P_{SH}\} \quad \text{or} \quad \left[S_{P-SV}\right]\{u_{P-SV}\} = \{P_{P-SV}\} \tag{18}$$

where $\{u_{SH}\}$, $\{u_{P\text{-}SV}\}$ and $\{P_{SH}\}$, $\{P_{P\text{-}SV}\}$ are the displacements and load vectors of the in-plane SH-wave and out-of-plane combined P- and SV-waves, respectively. $[S_{SH}]$ and $[S_{P\text{-}SV}]$ denote the out-of-plane and in-plane total dynamic-stiffness matrices of the offshore site, respectively. For the in-plane motions, $[S_{P\text{-}SV}]$ can be obtained by assembling the derived dynamic-stiffness matrix of the seawater layer with those of the base rock and soil layers. The effect of seawater layer is neglected in the calculation of $[S_{SH}]$ since the S-wave cannot transmit in seawater. $[S_{SH}]$ can be directly obtained by assembling the out-of-plane dynamic-matrices of the base rock and soil layers as proposed by Wolf [12].

The formulas for estimating the Poisson's ratio and P-wave velocity of porous soil suggested by Yang and Sato [8] are substituted into Eq. (18) to consider the effect of water saturation on the site amplification of seismic waves. It should be noted that the out-of-plane motion is not affected by the water saturation level of soil layers, since the pore water does not influence the propagation of S-wave [8]. By solving Eq. (18) in the frequency domain at every discrete frequency, the offshore site transfer functions, i.e., the ratios of seafloor motions to outcropping motions at any three directions, can be calculated.

4. Verification of the derived transfer function model

To verify the above derivations, the vertical transfer function of a rock site overlaid with a seawater layer is theoretically calculated. The total dynamic-stiffness matrix of the underwater rock site described above is obtained by assembling the dynamic-stiffness matrix of seawater layer (Eq. (17)) with that of the base rock. By solving the in-plane dynamic equilibrium equation at every discrete frequency, the vertical site transfer function, i.e., the

ratio of vertical motion at underwater base rock u_{zb} to outcropping vertical motion u_{zo} is derived as

$$H_z(\omega) = \frac{u_{zb}}{u_{zo}} = \frac{1}{1 + \dfrac{abs' \tan ksd}{(2kG^* - b)^2 + b^2 s't'} \cdot i} \tag{19}$$

and its modulus is

$$\left|H_z(\omega)\right| = \left|\frac{u_{zb}}{u_{zo}}\right| = \frac{1}{\sqrt{1 + \left[\dfrac{abs' \tan ksd}{(2kG^* - b)^2 + b^2 s't'}\right]^2}} \tag{20}$$

in which

$$a = \frac{K^* \omega}{l_x^W sc_p^{*W}} \quad \text{and} \quad b = kG^* \frac{1 + t'^2}{1 + s't'} \tag{21}$$

where the superscript W denotes the seawater layer; G^* is the shear modulus of base rock; s' and t' are the tangent values of incident angles of P- and SV-waves in the base rock, respectively.

It is evident that the modulus of the transfer function is always less than or equal to unity. The modulus tends to zero when tanksd approaches infinity, i.e.:

$$\tan ksd = \tan\left[\frac{2\pi f l_x^W}{c_p^{*W}}(-i)\sqrt{1 - \frac{1}{l_x^{W2}}} \cdot d\right] = \tan\left[\frac{2\pi fd}{c_p^{*W}} \sin\theta_p^W\right] \to \infty \tag{22}$$

where f denotes the frequency in Hz. Eq. (22) is satisfied when

$$f = f_n = n\frac{c_p^{*W}}{4d \sin\theta_p^W}, \ (n=1, 3, 5 \cdots) \tag{23}$$

where n is an odd number, f_n can be defined as the resonant frequencies of P-waves in seawater layer at which a destructive interference is induced by a phase change of P-wave motions at the water and base rock interface [2]. As a result, the vertical underwater motions will be significantly suppressed near the resonant frequencies of the seawater layer as compared to the vertical outcropping motions.

The derived vertical transfer function is compared with the models proposed by Crouse and Quilter [1] and Boore and Smith [2]. The former model is derived by assuming that the P-waves are vertically incident on an underwater base rock site and the S-waves are neglected; while the latter model is theoretically computed for different fault orientations by utilizing wavenumber integration method. To be consistent with these two studies, the depth of seawater layer and the incident angles of P- and SV-waves are assumed to be 60m and 90°, respectively. The schematic view of the base rock site overlaid with a seawater layer and the corresponding parameters are shown in Fig. 2.

As shown in Fig. 3, the derived vertical transfer function matches well with those proposed in the previous studies. The underwater vertical motion is significantly suppressed near the P-wave resonant frequency of 6.25 Hz. It is worth noting that the resonant frequency will be higher than 6.25 Hz if the P-waves are not vertically propagating in the seawater layer according to Eq. (23). Compared to the previous models, the effect of incident angle and the contribution of SV-waves can both be considered in the derived transfer function model. In other words, the previous models are special cases of the model proposed in the present study. Therefore, this model is believed capable of yielding more realistic representation of the

underwater site transfer functions as compared to the previous models. Moreover, the calculated transfer functions for a layered subsea site can be directly used in the simulation of seafloor seismic motions.

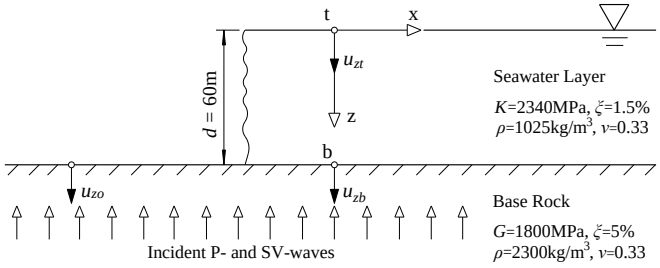

Fig. 2. A subsea base rock site for vertically incident P- and SV-waves

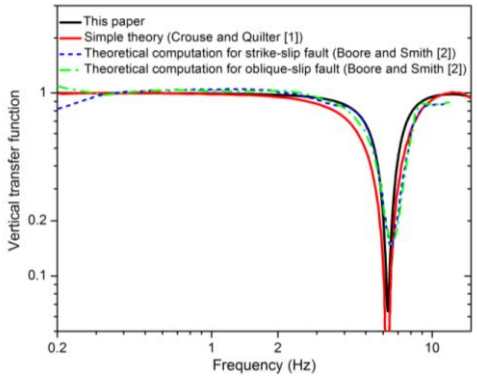

Fig. 3. Comparison of the proposed vertical transfer function model with those suggested in previous studies

5. Simulation of seafloor seismic motions

The seismological model of southwest Western Australia (SWWA) proposed by Hao and Guall [13] is employed to represent the seismic motions at the free surface of base rock. This model is obtained by modifying the eastern North America (ENA) model [17] to best fit the recorded strong ground motions in SWWA. To avoid repetition, the equations of SWWA seismological model are not given. More detailed information regarding this model can be found in [13].

Ground motion time histories on SWWA rock site corresponding to the upper bound event [13], namely Richter magnitude ML7.2 and epicentral distance 75 km, are stochastically simulated using the spectral representation method [18]. The Fourier amplitude spectra of outcropping motions can be obtained from the SWWA model. The phase angles of the simulated time histories are set to be random between 0 and 2π. The sampling frequency and upper cutoff frequency are set to be 100 Hz and 35 Hz, respectively. The time duration is estimated to be 25.2 s based on the model suggested in [17]. Moreover, the Jennings envelope function is utilized in the simulation to obtain nonstationary seismic motions.

Two typical onshore and offshore SWWA sites are selected to simulate seismic motions at respective sites, as shown in Fig. 4, in which d is the layer depth, G shear modulus, ρ density, ξ damping ratio, ν' Poisson's ratio of the soil skeleton, n porosity and S_r saturation degree. It should be noted that in the present study the Possion's ratio of soil skeleton of both the onshore and offshore site are assumed the same, but the actual Poisson's ratio of each porous soil layer depends not only on the soil skeleton Poisson's ratio but also on the water saturation level. The Poisson's ratio of porous soil increases with water saturation level [8, 9]. For the offshore site, the depth of seawater layer is assumed to be 80 m and the degree of saturation is higher than that of the onshore site. The incident angles of out-of-plane SH-wave

and in-plane P-wave are assumed to be 60°. Considering the effects of seawater layer and soil saturation, the onshore and offshore site transfer functions for the horizontal in-plane (X), horizontal out-of-plane (Y) and vertical in-plane (Z) motions are calculated and shown in Fig. 5. It can be observed that the transfer functions of horizontal out-of-plane motions are the same for the two sites because neither seawater nor soil saturation influences the propagation of SH-wave. However, for the in-plane motions with combined P- and SV-waves, the transfer functions of the offshore site are different from those of the onshore site, especially for the vertical in-plane motions dominated by P-wave. The seafloor vertical in-plane motion is significantly suppressed near the P-wave resonant frequencies of the seawater layer, i.e., 5.29 Hz, 15.88 Hz and 26.47 Hz as shown in Fig. 5.

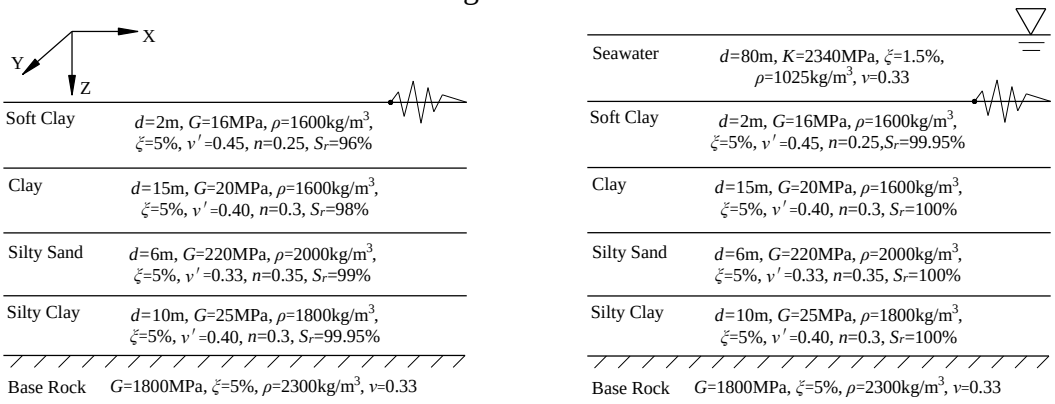

(a) Onshore site (b) Offshore site

Fig. 4. Example onshore and offshore sites in SWWA

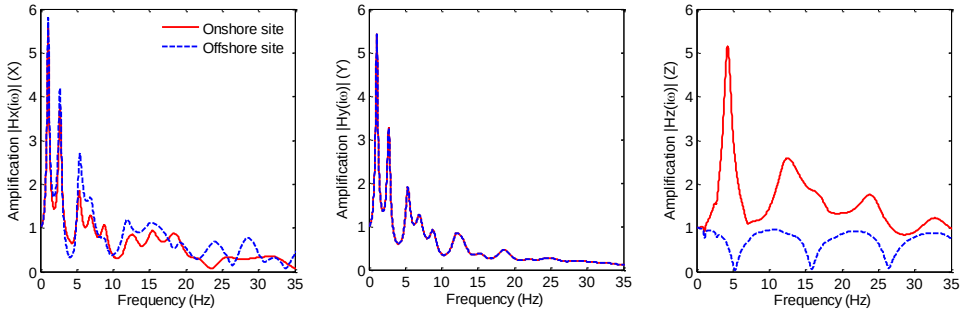

Fig. 5. Three-dimensional onshore and offshore site transfer functions

Considering linear elastic response only, the Fourier amplitude spectra of onshore and seafloor motions can be obtained by multiplying the SWWA model with the corresponding site transfer functions. The onshore and seafloor seismic motions are stochastically simulated using the calculated Fourier amplitude spectra and random phase angles. Four independent groups of three-dimensional seismic motions are simulated for each site. The PGAs, PGVs and the corresponding mean values of the generated seismic motions are summarized in Table 1. Fig. 6 plots a typical group of simulated three-dimensional acceleration time histories on different sites.

As summarized in Table 1, the two horizontal mean PGAs of simulated outcropping motions are 823 mm/s^2 and 855mm/s^2, which are comparable with the design PGA of 0.09g (882 mm/s^2) for Perth in SWWA [13]. The two horizontal mean PGAs of onshore motions are less than those of the outcropping motions. This is because most base rock ground motion energy concentrates in a frequency band higher than 5.0 Hz owing to SWWA intraplate source mechanism. The abundant horizontal outcropping motions with the frequencies higher than 5.5 Hz are deamplified, as can be observed from the onshore site transfer functions. It should be noted that previous studies also indicated that the SWWA soil sites amplify

horizontal rock motions in a frequency range up to 5 Hz, but deamplify those in the frequency higher than 5.0 Hz [13]. On the contrary, the vertical outcropping motion is significantly amplified by the onshore site even at frequencies up to 25.0 Hz as shown in Fig. 5. It should be noted that if the frequency contents of base rock motions are lower as usually observed in interpolate seismic motions, the horizontal ground motions would also be amplified. The mean PGVs of the simulated three-dimensional onshore motions are larger than those of the outcropping motions, due to the substantial site amplification effect at low frequency range.

Table 1. PGA and PGV values of the simulated seismic motions on different sites

Site	Base rock				Onshore site				Offshore site			
Group No.	G1	G2	G3	G4	G1	G2	G3	G4	G1	G2	G3	G4
Horizontal in-plane motion (x-component)												
PGA(mm/s^2)	845	827	799	820	493	479	503	487	520	507	552	537
PGV(mm/s)	11.9	13.7	11.2	12.4	25.0	15.8	17.4	20.3	25.1	21.6	20.3	22.8
Mean	823 mm/s^2		12.3 mm/s		491 mm/s^2		19.6 mm/s		529 mm/s^2		22.5 mm/s	
Horizontal out-of-plane motion (y-component)												
PGA(mm/s^2)	859	778	883	901	469	436	471	454	477	446	457	485
PGV(mm/s)	16.1	16.0	13.3	16.5	22.2	17.4	20.7	21.6	20.9	18.7	24.0	19.8
Mean	855 mm/s^2		15.5 mm/s		458 mm/s^2		20.5 mm/s		466 mm/s^2		20.9 mm/s	
Vertical in-plane motion (z-component)												
PGA(mm/s^2)	470	459	446	460	941	902	885	742	307	386	328	403
PGV(mm/s)	9.7	9.1	8.9	10.8	20.5	19.2	18.6	28.6	7.8	6.9	9.2	9.1
Mean	459 mm/s^2		9.6 mm/s		868 mm/s^2		21.7 mm/s		356 mm/s^2		8.3 mm/s	

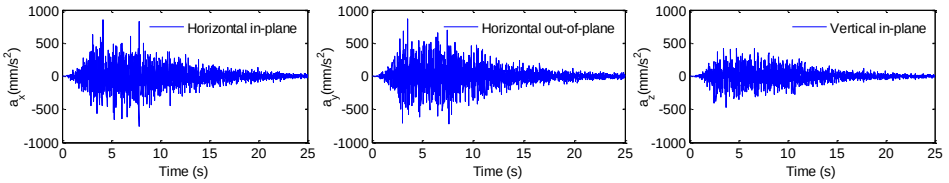

(a) Base rock free surface

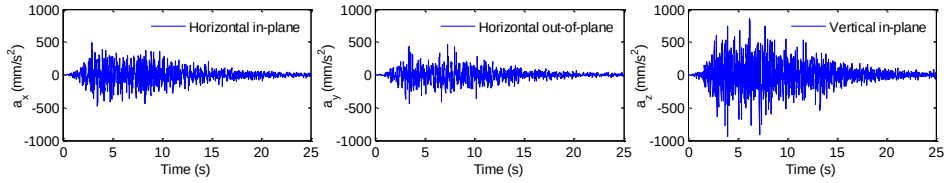

(b) Onshore site

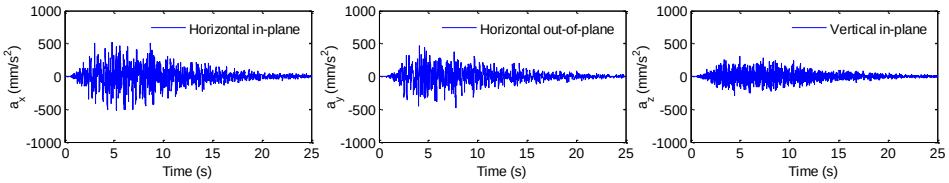

(c) Offshore site

Fig. 6. Simulated three-dimensional acceleration time histories on different sites

For the simulated seafloor motions, the horizontal PGA and PGV values are very close to those of the onshore motions because of the similar horizontal transfer functions as shown in Fig. 5. The most striking difference between the simulated onshore and seafloor motion is in the vertical in-plane motion. The seafloor vertical PGA and PGV are much smaller than the onshore ones, owing to the effects of seawater layer and soil saturation. The average vertical-to-horizontal (V/H) PGA ratio is 0.72 for the seafloor motions and 1.83 for the onshore motions, where the horizontal PGA is calculated by the geometric average of two horizontal PGA values. The characteristics of the simulated seafloor motions are consistent with the conclusions drawn from the analyses of seafloor earthquake recordings [2], namely,

the vertical component of seafloor seismic motions are significantly suppressed near the P-wave resonant frequencies of the seawater layer as compared to the onshore motions.

6. Conclusions

In this paper, the ground motion transfer functions for an offshore site are theoretically derived by considering the effects of seawater layer and soil saturation. Onshore and seafloor seismic motions are stochastically synthesized based on the SWWA seismological model and corresponding site transfer functions. The simulation results show that the difference is insignificant between the horizontal components of onshore and seafloor motions, while the vertical components of the seafloor motions are much weaker than those of the onshore motions. The simulated seafloor seismic motions are in line with the characteristics of available seafloor seismic records and can be utilized as inputs in the seismic analyses of offshore structures. It should be noted that the seafloor seismic motions can be simulated by combining the theoretically derived offshore site transfer functions with other stochastic ground motion attenuation models other than the SWWA model used in this study.

Acknowledgement

The authors acknowledge the financial support from the National Basic Research Program of China (No. 2011CB013605) and Australian Research Council Linkage Project LP110200906 for carrying out this research. The financial support from China Scholarship Council for the first author is also acknowledged.

References

1. Crouse CB, Quilter J. Seismic hazard analysis and development of design spectra for Maul A platform. In: Proceedings of Pacific conference on earthquake engineering. New Zealand; 1991. p. 137-48.
2. Boore DM, Smith CE. Analysis of earthquake recordings obtained from the Seafloor Earthquake Measurement System (SEMS) instruments deployed off the coast of southern California. Bull Seismol Soc Am 1999; 89(1): 260-74.
3. Sleefe GE. The long-term measurement of strong-motion earthquakes offshore southern California. In: Proceedings of the 22nd offshore technology conference. Houston; 1990. p. 561-68.
4. Biot MA. Theory of propagation of elastic waves in a fluid-saturated porous solid. I. Low-frequency range. J Acoust Soc Am 1956; 28(2): 168-78.
5. Biot MA. Theory of propagation of elastic waves in a fluid-saturated porous solid. II. Higher frequency range. J Acoust Soc Am 1956; 28(2): 179-91.
6. Vardoulakis I, Beskos DE. Dynamic behavior of nearly saturated porous media. Mech Mater 1986; 5: 87-108.
7. Verruijt A. Elastic storage of aquifers. In: Weist RJ, editor. Flow through porous media. New York: Academic Press; 1969. p. 331-76.
8. Yang J, Sato T. Interpretation of seismic vertical amplification observed at an array site. Bull Seismol Soc Am 2000; 90(2): 275-85.
9. Wang S, Hao H. Effects of random variations of soil properties on site amplification of seismic ground motions. Soil Dyn Earthq Eng 2002; 22(7): 551-64.
10. Versteeg HK, Malalasekera W. An introduction to computational fluid dynamics: the finite volume method. England: Pearson Education; 2007.
11. Batchelor GK. An introduction to fluid dynamics. Cambridge: Cambridge University Press; 2000.
12. Wolf JP. Dynamic soil-structure interaction. New Jersey: Prentice Hall Inc.; 1985.
13. Hao H, Gaull BA. Estimation of strong seismic ground motion for engineering use in Perth Western Australia. Soil Dyn Earthq Eng 2009; 29(5): 909-24.
14. Hatayama K. Theoretical evaluation of effects of sea on seismic ground motion. In: Proceedings of 13th world conference on earthquake engineering. Vancouver, Canada; 2004.
15. Jensen FB, Kuperman WA, Porter MB, Schmidt H. Computational ocean acoustics. London: Springer; 2011.
16. Lurton X. An introduction to underwater acoustics: principles and applications. New York: Springer; 2002.
17. Atkinson GM, Boore DM. Evaluation of models for earthquake source spectra in eastern North America. Bull Seismol Soc Am 1998; 88(4): 917-34.
18. Bi K, Hao H. Modelling and simulation of spatially varying earthquake ground motions at sites with varying conditions. Probab Eng Mech 2012; 29: 92-104.